

A Gapless Symmetry-Protected Topological Phase of Fermions in One Dimension

Anna Keselman and Erez Berg

Department of Condensed Matter Physics, Weizmann Institute of Science, Rehovot, Israel 76100

(Dated: March 4, 2022)

We consider a one-dimensional, time-reversal-invariant system with attractive interactions and spin-orbit coupling. Such a system is gapless due to the strong quantum fluctuations of the superconducting order parameter. However, we show that a sharply defined topological phase with protected, exponentially localized edge states exists. If one of the spin components is conserved, the protection of the edge modes can be understood as a consequence of the presence of a spin gap. In the more general case, the localization of the edge states arises from a gap to single particle excitations in the bulk. We consider specific microscopic models and demonstrate both analytically and numerically (using density matrix renormalization group calculations) that they can support the topologically non-trivial phase.

I. INTRODUCTION

Topological phases of matter are typically characterized by a gapped bulk spectrum, and protected gapless edge states with unique properties. The existence of a finite energy gap in the bulk plays a crucial role in the topological protection of the edge states. This therefore raises the question whether a topological phase, i.e. a phase with protected exponentially localized edges states, can exist in a gapless system [1].

Superconductors have been shown to host a variety of topological phases [2–7], depending on the symmetries and the dimensionality of the system. In one spatial dimension, such a phase hosts protected edge modes, termed Majorana bound states, which are in particular interesting due to their non-Abelian exchange statistics. Realization of this phase requires proximity coupling a one-dimensional system to a bulk three-dimensional superconductor [8–12]. In truly one-dimensional systems with intrinsic attractive interactions, strong quantum fluctuations of the superconducting order parameter leave the system gapless. E.g., this situation can arise if a quantum wire is coupled to a superconducting wire. It was shown that topological protection is then much weaker in general [13, 14] (the edge states are generically only power-law localized, rather than exponentially localized) and depends on the microscopics of the system [15].

In the presence of time-reversal symmetry a different kind of topological superconductors can be realized [16–26]. If the bulk is fully gapped, these phases host a Kramers pair of Majorana bound states [24, 27–29].

In this work, we show that one-dimensional time reversal symmetric systems can support a well-defined topological superconducting phase, even when the particle number is conserved. The two necessary ingredients to realize this phase are attractive effective interactions and spin-orbit coupling. We start by giving a field theoretical argument for the existence of the topological phase, distinct from a trivial one. We show that the boundary between the topological and the trivial phases hosts exponentially localized edge states and discuss their prop-

erties. The edges exhibit an anomalous relation between time reversal and the local fermion parity operator, just like in the fully gapped case. We then demonstrate the existence of the topological phase and its properties numerically. To this end we consider a simple model that exhibits a phase transition between the trivial and the topological phases and study it using the density matrix renormalization group (DMRG) technique. Finally, we consider a system consisting of a semiconducting wire with spin-orbit coupling and repulsive interactions coupled to a superconducting wire, and show using bosonization and weak coupling renormalization group (RG) that it can be driven into the gapless topological phase.

II. FIELD THEORY OF GAPLESS TIME-REVERSAL-INVARIANT TOPOLOGICAL SUPERCONDUCTORS

A. Spin conserving case

We begin by considering an interacting, time reversal invariant one-dimensional electron gas (1DEG), described at low energies as a Luttinger liquid. In bosonized language, the Hamiltonian can be written as

$$H_0 = \sum_{\alpha=\rho,\sigma} \frac{u_\alpha}{2\pi} \int \left(K_\alpha (\partial_x \theta_\alpha)^2 + \frac{1}{K_\alpha} (\partial_x \phi_\alpha)^2 \right) dx, \quad (1)$$

where ρ, σ correspond to the charge and spin degrees of freedom, $\rho(x) = -\frac{1}{\pi} \partial_x \phi_\rho$ and $s^z(x) = -\frac{1}{2\pi} \partial_x \phi_\sigma$ are the charge and spin densities, respectively, and $\frac{1}{\pi} \theta_\alpha$ is the field conjugate to ϕ_α , $[\phi_\alpha(x), \theta_\alpha(x')] = i\pi \Theta(x' - x)$, where $\Theta(x)$ is the Heaviside step function.

The relation to fermionic operators, describing modes linearized around the Fermi momentum k_F , is given by

$$R(L)_s = \frac{U_s}{\sqrt{2\pi a}} e^{-i(\pm \frac{1}{2} \phi_\rho - \theta_\rho + s(\pm \frac{1}{2} \phi_\sigma - \theta_\sigma))}. \quad (2)$$

where s denotes the spin of the fermion, U_s are the Klein factors that impose the anti-commutation relations between the different spin species, $+$ ($-$) signs correspond

to $R(L)$, representing right(left) movers, respectively, and a is the short distance cutoff in the theory [30]. Back-scattering processes give rise to cosine terms that can gap out some of the modes in the system. We assume the system to be at a generic filling, such that there are no relevant umklapp processes.

Our system is symmetric under time-reversal (TR) symmetry, denoted by \mathcal{T} (class DIII in the Zirnbauer-Altlund classification [31], such that $\mathcal{T}^2 = -1$). Under time reversal, $R_\uparrow \rightarrow L_\downarrow$, $L_\downarrow \rightarrow -R_\uparrow$, $L_\uparrow \rightarrow R_\downarrow$, and $R_\downarrow \rightarrow -L_\uparrow$. These relations correspond to the following transformations of the bosonic fields: $\theta_\rho \rightarrow -\theta_\rho$, $\phi_\rho \rightarrow \phi_\rho$, $\theta_\sigma \rightarrow \theta_\sigma$, $\phi_\sigma \rightarrow -\phi_\sigma$, $U_\uparrow \rightarrow U_\downarrow$, and $U_\downarrow \rightarrow -U_\uparrow$. These transformation rules reproduce the correct behavior of the spin and charge densities and currents under TR.

We consider a system with spin-orbit coupling, and hence no $SU(2)$ spin symmetry. Let us assume, for simplicity, that the spin is conserved along one direction (e.g. the z direction, such that S_z is conserved). This condition will be relaxed later on. The most general four-fermion back-scattering interaction consistent with time-reversal symmetry is

$$g \left(R_\uparrow^\dagger L_\uparrow L_\downarrow^\dagger R_\downarrow + h.c. \right) = \frac{g}{2\pi^2 a^2} \cos(2\phi_\sigma), \quad (3)$$

where the coupling g is a real number. Note that such a cosine term is invariant under \mathcal{T} , according to the transformation rule of ϕ_σ above. (Higher order processes are also possible, but are less relevant in the RG sense.) If this cosine term is relevant, it opens a spin gap, driving the system into a ‘‘Luther-Emery phase’’ [32] with only one gapless (charge) mode. The sign of g determines the nature of the resulting phase. To understand this recall that the spin-singlet and spin-triplet pairing order parameters are given by

$$\begin{aligned} O_{SS} &= R_\uparrow^\dagger L_\downarrow + L_\uparrow^\dagger R_\downarrow \propto U_\uparrow U_\downarrow e^{-2i\theta_\rho} \cos(\phi_\sigma), \\ O_{TS}^z &= R_\uparrow^\dagger L_\downarrow - L_\uparrow^\dagger R_\downarrow \propto U_\uparrow U_\downarrow e^{-2i\theta_\rho} \sin(\phi_\sigma), \end{aligned} \quad (4)$$

while the spin-density wave and charge-density wave order parameters are given by

$$\begin{aligned} O_{CDW} &= R_\uparrow^\dagger L_\uparrow + L_\downarrow^\dagger R_\downarrow \propto e^{-i\phi_\rho} \cos(\phi_\sigma), \\ O_{SDW}^z &= R_\uparrow^\dagger L_\uparrow - L_\downarrow^\dagger R_\downarrow \propto e^{-i\phi_\rho} \sin(\phi_\sigma). \end{aligned} \quad (5)$$

For $g < 0$, the cosine term pins the field ϕ_σ to zero (or equivalently to any integer multiple of π , i.e. πn with $n \in \mathbb{Z}$), resulting in the dominant superconducting correlations being of the spin-singlet order parameter. (As the charge sector remains gapless, these pairing correlations decay with a power law dictated by the Luttinger parameter K_ρ and no true long range order can develop). For $g > 0$, ϕ_σ is pinned to $\pi(n + \frac{1}{2})$, where $n \in \mathbb{Z}$, and the dominant superconducting correlations are now of the spin-triplet order parameter. These two cases correspond

to two distinct phases; in order to go between them without breaking time-reversal symmetry, the coupling g has to cross zero, resulting in the closing of the spin gap [33]. We refer to these phases as *trivial* and *topological* respectively, in analogy with the fully gapped case. When the superconducting order parameter is conventional s-wave, we expect the system to be in the trivial phase, while for a p-wave order parameter the system is topological. This identification is in agreement with the vacuum being in the trivial phase, as a large back-scattering potential at the end of the system pins ϕ_σ to zero.

The phase diagram of an interacting 1DEG with spin-orbit coupling, and the possibility of a phase with dominant triplet superconducting correlations was discussed in Refs. [34, 35], where it was demonstrated how this phase can arise in a model that describes certain quasi-one-dimensional organic conductors. However, to the best of our knowledge, the topological nature of this phase (manifested in its protected edge modes, as we argue below) has not been discussed.

Consider an edge of a topological system, or equivalently a boundary between a trivial and a topological phase. Since the field ϕ_σ is pinned to πn_1 on one side of the boundary and to $\pi(n_2 + \frac{1}{2})$ on the other, where $n_{1,2}$ are integers, there must be a kink of minimal magnitude $\pm \frac{\pi}{2}$ in ϕ_σ across the boundary. Such a kink in ϕ_σ corresponds to an accumulation of spin:

$$S_z = \int s^z(x) dx = - \int \frac{1}{2\pi} \partial_x \phi_\sigma dx = \pm \frac{1}{4}, \quad (6)$$

i.e. half the spin of an electron. The same ‘‘fractional spin’’ appears at the edge of a time-reversal invariant fully gapped topological superconductor [24].

The lowest energy configurations of ϕ_σ for a topological system of finite size are shown in Fig. 1. The two configurations plotted in blue solid lines correspond to an even number of particles in the system with total $\langle S_z \rangle = 0$. These configurations are degenerate up to a splitting exponential in system size, as in the case of a fully gapped topological superconductor with time-reversal symmetry. Adding a single particle in the bulk of the system requires creating a kink of magnitude $\pm\pi$ (as the extra particles carries spin $S_z = \pm \frac{1}{2}$). Such a kink costs a finite amount of energy. Adding a particle near the edge, however, only requires flipping the direction of the $\frac{\pi}{2}$ kink at that edge without an extra energy cost. Since the number of particles in the system is a good quantum number, adding a particle costs charging energy, but this contribution decreases with the system size L as $\frac{1}{L}$. The resulting configurations with an odd number of particles and total $\langle S_z \rangle = \pm \frac{1}{2}$ are given by red dashed lines in Fig. 1. (Note that the two states with an odd number of particles are exactly degenerate, in accord with Kramers’ theorem.) We therefore expect that the gapless topological phase will host single particle edge excitations which cost zero energy in the thermodynamic limit. This is in

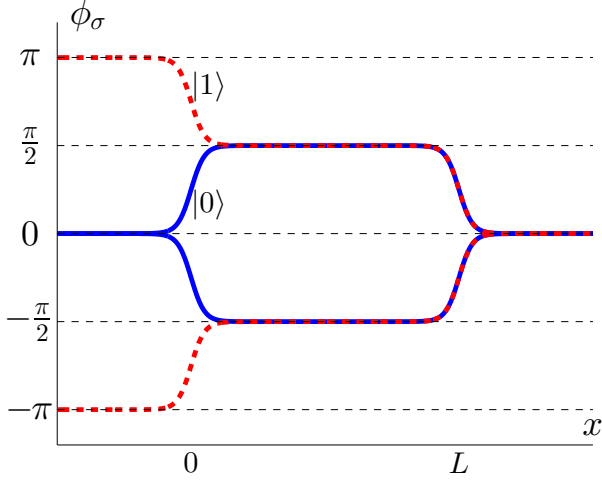


FIG. 1: Low energy configurations of ϕ_σ in a finite size gapless topological superconductor. Configurations plotted in red dashed lines correspond to total spin of $\pm\frac{1}{2}$ in the system, i.e. odd number of particles, while configurations plotted in blue solid lines correspond to zero total spin, i.e. even number of particles. To calculate the local tunneling density of states we calculate the matrix element of a single particle creation operator $\Psi_\dagger^\dagger(x)$ between the states denoted by $|0\rangle$ and $|1\rangle$.

sharp contrast to the gapless trivial phase where no such edge excitations exist.

This distinction can be seen in Fig. 2, depicting the ground state energy of a system with open boundary conditions as a function of the number of particles in the two cases. For a system in the trivial phase, states with an odd number of particles lie on a parabola separated by Δ , the single particle gap in the system, from the states with an even number of particles. For a system in the topological phase, an extra particle can be added at the edge of the system at a cost of the charging energy only. The two states are distinguished by the pair binding energy in the system

$$E_B = E_{2N+1} - \frac{1}{2}(E_{2N+2} + E_{2N}) \quad (7)$$

as the size of the system is varied. Extrapolating to the infinite system size limit, we expect to obtain the single particle gap, $\lim_{L \rightarrow \infty} E_B = \Delta > 0$, if the system is in the trivial phase. If the system is in the topological phase and with open boundary conditions, we expect $\lim_{L \rightarrow \infty} E_B$ to be zero. In contrast, in a system with periodic boundary conditions, both phases are characterized by a finite E_B in the thermodynamic limit.

Experimentally, the existence of a low energy single particle edge state is reflected in the local tunneling den-

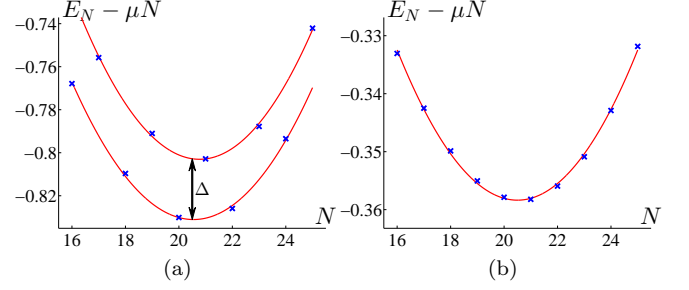


FIG. 2: The ground state energy of a system with open boundary conditions as the number of particles is varied for (a) a system in the trivial phase (b) a system in the topological phase. In both cases the contribution of the chemical potential is subtracted, Δ indicates the single particle gap. In the topological phase a low energy state appears for an odd number of particles due to the presence of the low energy edge state. Note that a single particle gap is still present in the bulk of the system. The data is obtained using DMRG study of the model given by Eq. 16 for a system of length $L = 100$ sites with model parameters $t = 1$, $U = -1$ and spin-orbit coupling $v = 1$ in (a) and $v = 0$ in (b). The chemical potential that is subtracted in both cases is found from a linear fit of E_N to N . The red solid lines are fits to parabolas. The finite curvature of the parabolas is due to the charging energy, and depends on the size of the system.

sity of states (TDOS)

$$\frac{1}{\pi} \text{Im} G^R(\omega, x) = \sum_{n,s} \delta(\omega - \omega_n) \left(|\langle 0 | \Psi_s^\dagger(x) | n \rangle|^2 + |\langle 0 | \Psi_s(x) | n \rangle|^2 \right), \quad (8)$$

in the $\omega \rightarrow 0$ limit. Here $|0\rangle$ denotes the ground state of the system and $|n\rangle$ an excited state at energy $\hbar\omega_n$. Assuming the number of particles in the ground state is even, the configuration of ϕ_σ in this state is given by one of the blue solid curves in Fig. 1, e.g. the one denoted by $|0\rangle$. The lowest energy excited state that contributes to the sum in Eq. 8 corresponds to a configuration of ϕ_σ denoted by $|1\rangle$. Using the bosonized representation of $\Psi_s^\dagger(x)$ and a mode expansion for the bosonic fields, $\phi_{\rho,\sigma}$ and $\theta_{\rho,\sigma}$, we obtain for the matrix element:

$$|\langle 1 | \Psi_\dagger^\dagger(x) | 0 \rangle|^2 \sim \left(\frac{a}{L} \right)^{\frac{1}{K_\rho}} \left(\frac{a}{x} \right)^{\frac{\alpha}{2}} e^{-\frac{\pi}{2K_\sigma} \frac{x}{\xi}}, \quad (9)$$

where $\alpha = \frac{1}{K_\rho} + \frac{1}{4}K_\rho$, Δ_σ is the spin gap, and $\xi = \frac{v_\sigma}{\Delta_\sigma}$ is the correlation length in the spin sector. For details of the calculation see Appendix A.

B. Non-spin conserving case

We now generalize the analysis of the previous section to the more generic case, in which none of the spin components are conserved.

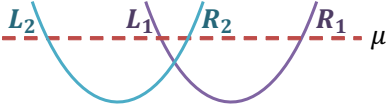


FIG. 3: Generic spectrum for a system without inversion symmetry. $R(L)_{1,2}$ denote the right(left) movers in each band. Under time-reversal symmetry $R_1 \rightarrow L_2$ and $R_2 \rightarrow -L_1$.

Let us first consider a case where the system has no inversion center. Then, the single particle spectrum is generically of the form shown in Fig. 3. We linearize the modes close to Fermi energy and denote by $R(L)_{1,2}$ the right (left) movers in each band. Under time-reversal symmetry $R_1 \rightarrow L_2$ and $R_2 \rightarrow -L_1$. We can therefore assign a pseudo-spin \uparrow, \downarrow to the two bands, respectively, and write the linearized fermionic modes in terms of the bosonic fields $\phi_{\rho,\sigma}$ and $\theta_{\rho,\sigma}$ exactly as before, where ϕ_σ is now related to the density of the pseudo-spin. The only four-particle back-scattering term allowed by time-reversal symmetry is $R_1^\dagger L_1 L_2^\dagger R_2 + h.c.$, or $\cos(2\phi_\sigma)$ in terms of the bosonic fields, and all the analysis presented for the S_z conserving case still holds.

If the system has an inversion center, the resulting phase diagram is richer. The case of spin anisotropic interactions in an inversion symmetric system with time-reversal symmetry was analyzed in [35]. Here, we outline this analysis briefly, and comment on the topological nature of the various phases and their boundary properties.

After an appropriate rotation in spin space, the most general four-fermion inversion symmetric interaction can be written as

$$H_{\text{int}} = g_s \Delta_s^\dagger \Delta_s + \sum_{\hat{d}=\hat{x},\hat{y},\hat{z}} g_{\hat{d}} \Delta_{\hat{d}}^\dagger \Delta_{\hat{d}}, \quad (10)$$

where $\Delta_s = L^T (i s^y) R$ is a singlet order parameter, $\Delta_{\hat{d}} = L^T (i s^y \hat{d} \cdot \vec{s}) R$ is a time-reversal symmetric triplet order parameter characterized by the orientation of a headless \hat{d} vector, and we have dropped terms that do not couple the right and left movers. Here $L(R)$ are spinors in spin space, $L(R)^T = (L(R)_\uparrow, L(R)_\downarrow)$. Note that inversion symmetry prohibits cross terms that couple the singlet and triplet order parameters.

The back-scattering part of this interaction can be written in terms of the bosonic fields as

$$H_{\text{int}} = \frac{1}{2\pi^2 a^2} \{ (g_z - g_s) \cos(2\phi_\sigma) + (g_{\hat{y}} - g_{\hat{x}}) \cos(4\theta_\sigma) \}. \quad (11)$$

The resulting phase diagram hosts four phases with dominant superconducting correlations. These correspond to pinning of either ϕ_σ or θ_σ with two possible values for each, depending on the sign of $(g_z - g_s)$ or $(g_{\hat{y}} - g_{\hat{x}})$, respectively. Let us denote the phase in which $\phi_\sigma = 0$ by SS (dominant singlet superconducting correlations), and the phase with $\phi_\sigma = \pm \frac{\pi}{2}$ by TS_z (dominant triplet

correlations with $\hat{d} \parallel \hat{z}$). The other two phases with $\theta_\sigma = n\frac{\pi}{2}, (n + \frac{1}{2})\frac{\pi}{2}$ will be denoted as TS_x and TS_y , respectively.

The SS and TS_z phases are exactly the ones discussed in the context of an S_z conserving system. These phases are distinct from each other (in the sense that they cannot be adiabatically connected without a phase transition in which the gap in the spin sector closes) as long as time reversal symmetry is preserved. Below, we argue that the $\text{TS}_{x,y,z}$ can be adiabatically connected to each other without breaking time reversal symmetry. However, they are distinct as long as certain mirror symmetries, $M_{x,y,z}$ (where M_x is a mirror symmetry that takes $x \rightarrow -x$, etc.) are maintained; in the presence of such a mirror symmetry, an interface between a pair of TS phases with different spin quantization axes hosts protected edge states.

To see that the TS_x and TS_y can be adiabatically connected without TR symmetry breaking, consider the following family of interaction Hamiltonians: $H'_{\text{int}}(\alpha) = -|g'| \Delta_{\hat{d}}^\dagger \Delta_{\hat{d}}$, where $\hat{d} = \cos(\alpha)\hat{x} + \sin(\alpha)\hat{y}$. In bosonized form, $H'_{\text{int}}(\alpha) \propto -|g'| \cos(4(\theta_\sigma - \alpha/2))$; therefore, as α varies from 0 to $\frac{\pi}{2}$, the value to which θ_σ is pinned changes from 0 to $\frac{\pi}{4}$, the values that correspond to the TS_x and TS_y phases, respectively. Interpolating from the TS_x or TS_y phases to the TS_z phase is more difficult in the context of Abelian bosonization; nevertheless, by a rotation in spin space we can show that these phases can also be adiabatically connected in a similar fashion.

Note, however, that this path in Hamiltonian space defined above includes terms like $\Delta_{\hat{x}}^\dagger \Delta_{\hat{y}}$, that break M_x and M_y . In the presence of either of these mirror symmetries, such terms are forbidden, and the TS_x and TS_y phases are distinct from each other.

In order to understand the topological nature of the TS_x and TS_y phases, we examine the low energy spectrum in a system with open boundary conditions. Let us consider a system of length L , with boundary conditions imposed by a strong back-scattering potential at both ends. The back-scattering term has the form

$$-|V_b| \sum_{s=\uparrow,\downarrow} R_s^\dagger L_s + h.c. = -\frac{2|V_b|}{\pi a} \cos(\phi_\rho) \cos(\phi_\sigma). \quad (12)$$

Such a potential pins both ϕ_ρ and ϕ_σ to either an even or an odd multiple of π at both ends of the system, $x = 0$ and L . A system described by a state with θ_σ pinned to a specific value in the bulk can not satisfy these boundary conditions, due to the non-trivial commutation relations $[\phi_\sigma(0), \theta_\sigma(x)] = i\pi$, where $0 < x < L$.

Moreover, the fermion parity $\mathcal{P} = e^{i\pi N}$, where $N = -\frac{1}{\pi}(\phi_\rho(L) - \phi_\rho(0))$ is the total number of particles, is not well defined in such a state. To see this note that using the boundary conditions dictated by Eq. 12, we can rewrite \mathcal{P} in terms of the spin degrees of freedom as

$$\mathcal{P} = e^{-i(\phi_\sigma(L) - \phi_\sigma(0))}, \quad (13)$$

since $(\phi_\rho(L) - \phi_\rho(0)) = (\phi_\sigma(L) - \phi_\sigma(0)) \bmod 2\pi$. Therefore, the following anti-commutation relations hold $\mathcal{P}e^{i\theta_\sigma(x)} = -e^{i\theta_\sigma(x)}\mathcal{P}$.

Ground states of the, e.g. TS_x phase, with well defined fermion parity can be constructed in the following way: $|\psi_{0,\pm}\rangle = |\theta_\sigma = 0\rangle \pm |\theta_\sigma = \pi\rangle$ and $|\psi_{\frac{\pi}{2},\pm}\rangle = |\theta_\sigma = \frac{\pi}{2}\rangle \pm |\theta_\sigma = \frac{3\pi}{2}\rangle$, where the symmetric (anti-symmetric) superpositions correspond to even (odd) fermion parity states. (Recall that all the states $|\theta_\sigma = n\frac{\pi}{2}\rangle$ are degenerate in the bulk.) Note also that these two sets of states are distinct and are related by a transformation that transfers a single fermion between the two edges, $\Psi_s^\dagger(L)\Psi_s(0) \sim e^{\pm\frac{i}{2}[\phi_\sigma(L)\pm\phi_\sigma(0)]}$. This is reminiscent of the four-fold ground state degeneracy present in the fully gapped time-reversal-symmetric topological phase, linked to the existence of a low energy single particle excitation at the edge of the system. In our gapless system, however, states with a different total fermion parity also differ in their particle number, and hence are not degenerate; a system with a given particle number has only two ground states, given *e.g.* by $|\psi_{0,+}\rangle$ and $|\psi_{\frac{\pi}{2},+}\rangle$.

C. Symmetry fractionalization at the edges

To better understand the nature of the topological phase, we consider the connection between time reversal and the local fermion parity at its edges. In fully gapped systems, symmetry-protected topological phases are characterized by a projective (fractionalized) representation of the symmetry operators when acting on the low-energy states of the edge [36–41]. In the case of a time-reversal symmetric topological superconductor, there is an anomalous relation between time reversal and fermion parity at the edge: $\mathcal{T}\mathcal{P}_{R,L} = -\mathcal{P}_{R,L}\mathcal{T}$, where $\mathcal{P}_{R,L}$ is the *local* fermion parity operator acting on the right or left ends of the system, respectively [16, 42]. These are local operators acting near the two edges, defined such that in the low-energy subspace the total fermion parity operator has the form $\mathcal{P} = \mathcal{P}_L\mathcal{P}_R$. We will show that, even though our system is gapless, the gap to single fermion excitations in the bulk guarantees that a similar decomposition of fermion parity in terms of local edge operators holds; therefore, the topological phase is characterized by the same anomalous relation between time reversal and fermion parity as in the mean-field case.

For concreteness, we demonstrate this for a system in the TS_z phase. In the low energy subspace, the total fermion parity given by Eq. 13 can be written as a product of local fermion parities at the edges of the system with

$$\begin{aligned}\mathcal{P}_L &= ie^{-i(\phi_\sigma(x_1) - \phi_\sigma(0))}, \\ \mathcal{P}_R &= -ie^{-i(\phi_\sigma(L) - \phi_\sigma(x_2))},\end{aligned}\quad (14)$$

where $x_{1,2}$ are arbitrary points within the bulk of the system, a few correlation lengths away from the left and right edge, respectively. We have used the fact that $\langle e^{-i(\phi_\sigma(x_2) - \phi_\sigma(x_1))} \rangle = 1$, since ϕ_σ is pinned to a constant value in the bulk. The phase of the parity operators was chosen such that $\mathcal{P}_R^2 = \mathcal{P}_L^2 = 1$. (Recall that at the boundary of the system ϕ_σ is pinned to an integer multiple of π , while in the bulk it is pinned to $\pi(n + \frac{1}{2})$; hence $\phi_\sigma(x_1) - \phi_\sigma(0) = \phi_\sigma(L) - \phi_\sigma(x_2) = \frac{\pi}{2} \bmod \pi$.) Since the time-reversal operator \mathcal{T} is anti-unitary and takes ϕ_σ to $-\phi_\sigma$, we obtain $\{\mathcal{T}, \mathcal{P}_{R,L}\} = 0$.

For a system in the trivial phase, a consistent phase choice for the parity operators that ensures $\mathcal{P}_R^2 = \mathcal{P}_L^2 = 1$ is

$$\begin{aligned}\mathcal{P}_L &= e^{-i(\phi_\sigma(x_1) - \phi_\sigma(0))}, \\ \mathcal{P}_R &= e^{-i(\phi_\sigma(L) - \phi_\sigma(x_2))},\end{aligned}\quad (15)$$

giving the usual commutation relations $[\mathcal{T}, \mathcal{P}_{R,L}] = 0$.

III. NUMERICAL EVIDENCE FOR THE EXISTENCE OF A TOPOLOGICAL PHASE

We next demonstrate the existence of the topological phase in a simple model, using the density matrix renormalization group (DMRG) [43–46].

Consider spinful electrons on a 1D lattice, with spin-orbit coupling in an alternating direction and spin-anisotropic interactions that explicitly favor triplet pairing

$$\begin{aligned}H &= H_0 + H_{\text{soc}} + H_{\text{int}} \\ H_0 &= -t \sum_{j,s=\uparrow,\downarrow} c_{j,s}^\dagger c_{j+1,s} + h.c. \\ H_{\text{soc}} &= iv \sum_{j,s,s'=\uparrow,\downarrow} c_{j,s}^\dagger \left(\frac{1+(-1)^j}{2} s_{s,s'}^z + \frac{1-(-1)^j}{2} s_{s,s'}^x \right) c_{j+1,s'} + h.c. \\ H_{\text{int}} &= U \sum_j \Delta_j^\dagger \Delta_j, \quad \Delta_j = c_{j,\uparrow} c_{j+1,\downarrow} + c_{j,\downarrow} c_{j+1,\uparrow},\end{aligned}\quad (16)$$

where t is the hopping amplitude along the chain, v is the spin-orbit coupling strength and U is the interaction strength.

In the absence of the single-particle spin-orbit coupling, i.e. for $v = 0$, the \hat{z} component of the spin is conserved. For any $U < 0$ a spin gap opens and we expect to find the system in the topological phase. The spin-orbit coupling term is chosen such that it breaks spin symmetry completely. We will use it to study the robustness of the topological phase without spin conservation, and its range of stability.

We calculated the low energy spectrum for a system of length $L = 100$ with $N = 20$ particles and open boundary conditions. The parameters used in this calculation are $t = 1$, $U = -1$, $v = 0$. The ground state is two-fold degenerate, as expected in the topological phase. We could

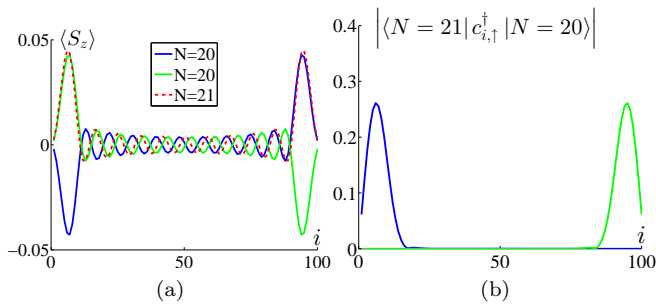


FIG. 4: DMRG results for the model described by Eq. 16 in absence of spin-orbit coupling, $v = 0$. A system of length $L = 100$ sites with model parameters $t = 1$, $U = -1$ is considered. (a) Expectation value of the \hat{z} component of the spin along the chain in the ground states of the system for even and odd number of particles. The blue and green solid curves correspond to the two degenerate ground states of a system with $N = 20$ particles and zero net spin. Accumulation of spin at the edge of the system is observed, with the integrated spin in the left (right) half of the system being $\pm \frac{1}{4}$. The red dashed curve corresponds to the ground state of a system with $N = 21$ particles and total spin $S = +\frac{1}{2}$. Due to the non-zero spin localized at the edge, and power-law decaying spin density wave correlations expected in a phase with ϕ_σ pinned to $\frac{\pi}{2}$ (see Eq. 5), a spin density wave pattern is formed in the bulk. (b) Matrix elements for the transition between each of the two ground states with $N = 20$ particles and the ground state with $N = 21$ particles by adding a spin up particle at a position i along the lattice. As can be seen, the matrix elements are non-zero only at either end of the system depending on the initial state. This is in agreement with the existence of low energy single particle states at the edges of the system.

not resolve the expected exponential splitting between the two lowest energy states; this is presumably because the correlation length is much smaller than the system size. The two states found by DMRG are the minimally entangled states with an integrated spin of $\langle S_z \rangle = \pm \frac{1}{4}$ near the two edges. The configuration of the \hat{z} component of the spin in the two ground states is shown in Fig. 4a. The topological phase is expected to have power-law decaying spin density wave correlations in the bulk (see Eq. 5 for ϕ_σ pinned to $\frac{\pi}{2}$). As a result, the spin polarization at the edge induces a spin density wave that decays as a power law into the system, clearly visible in the figure.

We then obtain the lowest energy state of the system with an extra spin up particle. Let us denote it by $|2N + 1\rangle$. We calculate the matrix elements between each of the states with an even number of particles, $|2N\rangle$, to the state $|2N + 1\rangle$ by adding a spin up particle at a position i along the lattice, $|\langle 2N + 1 | c_{i,\uparrow}^\dagger | 2N \rangle|$ (see Fig. 4b). We find that the matrix elements are non-zero only at either end of the system, depending on the initial state. This is in agreement with the existence of a low energy

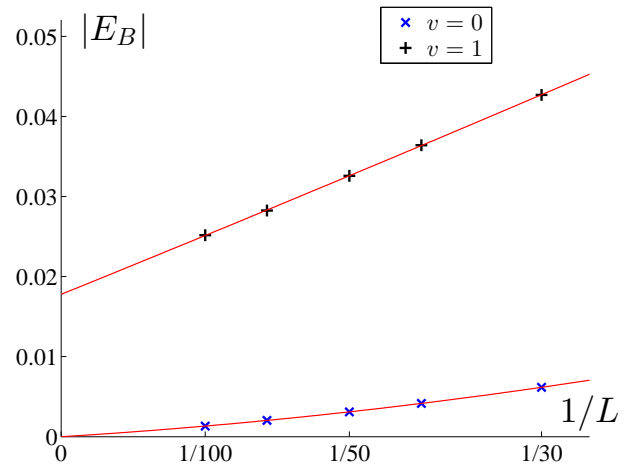


FIG. 5: Pair binding energy (see Eq. 7) as function of system size for the model Hamiltonian given in Eq. 16 with parameters $t = 1$, $U = -1$, spin-orbit couplings $v = 0$ and $v = 1$, and fixed density $n = \frac{2N}{L} = 0.2$. The red solid lines are fits to parabolic curves. For $v = 0$ the system is in the topological phase and the pair binding energy tends to zero as $1/L \rightarrow 0$. For $v = 1$ the system is in the trivial phase and E_B tends to a finite constant equal to the single particle gap in the system.

single particle state at the edge of the system.

In addition we calculated the pair binding energy (defined in Eq. 7 above), as function of system size, keeping the density of particles fixed at $n = 0.2$ (see Fig. 5). We find that it indeed tends to zero as the system becomes large, as expected in the topological phase. This once again indicates the existence of a low energy edge state, with an energy going to zero in the thermodynamic limit.

For non-zero v , S_z is no longer conserved. Moreover, conservation of S_z (or any other spin component) mod 2 is also broken, ensuring no residual symmetries are present. However, we find that the system remains in the topological phase for a finite range of spin-orbit coupling strength, $v < v_c$. To see this, we perform finite-size scaling of the energy gap (defined as the energy difference between the first excited state and the ground state in an even particle number sector); keeping the density constant, we choose system sizes for which the number of particles is even. We find the gap to be exponentially decreasing with system size, as expected in the topological phase. For each spin-orbit coupling strength, we extract the inverse correlation length in the system by fitting the energy gap, ΔE , vs. system size, L , to the form $\Delta E = \frac{1}{L} e^{-L/\xi}$. We find that the correlation length ξ diverges as v approaches $v_c \approx 0.22$ (see Fig. 6).

For $v \gtrsim v_c$ we calculate the pair binding energy, E_B , for different system sizes. As can be seen from Fig. 6, the binding energy tends to a non-zero value that increases with v , as the system size is increased (see also Fig. 5 for E_B as function of system size for $v = 1$). This indicates

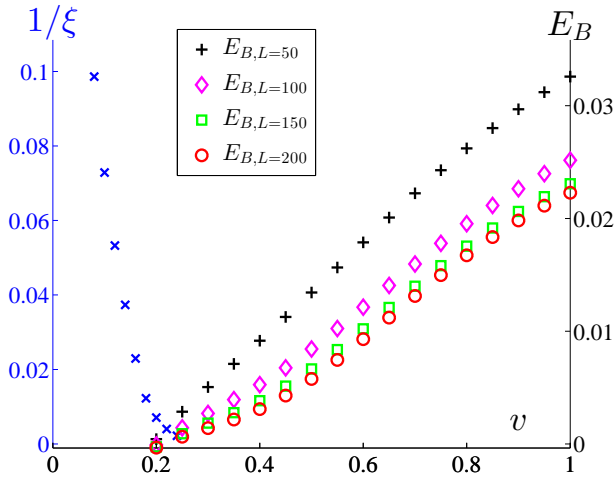


FIG. 6: Phase diagram obtained for the model described by Eq. 16 with model parameters $t = 1$, $U = -1$ and total particle density $n = \frac{N_{\uparrow} + N_{\downarrow}}{L} = 0.2$. As the spin-orbit coupling strength is increased, a phase transition from the topological to the trivial phase is observed. For $v < v_c \approx 0.22$ the gap (defined as the energy difference between the first excited state and the ground state) in a system with an even number of particles decreases exponentially with the system size, as expected for the topological phase. Data points marked by a blue cross correspond to the inverse correlation length obtained from the finite size scaling of the gap $\Delta E = \frac{1}{L} e^{-L/\xi}$. For $v > v_c$ we plot the pair binding energy, E_B (see Eq. 7), for different system sizes. In the limit $L \rightarrow \infty$ the pair binding energy tends to a non-zero value, increasing with v , indicating an opening of a trivial single particle gap in the system.

the opening of a single particle gap and the absence of edge states in the trivial phase, as discussed in the previous section.

To emphasize the difference between the trivial and the topological phases, we calculate the ground state energy of the system, as the number of particles is varied in each phase (see Fig. 2). For $v = 1 > v_c$, the system is in the trivial phase with odd particle number states having energy larger by Δ , the single particle gap, with respect to the states with an even number of particles. For $v = 0 < v_c$ the system is in the topological phase and there is no gap for single particle excitations; the extra particle can be accommodated at low energy at the edges.

IV. POSSIBLE REALIZATION OF THE TOPOLOGICAL PHASE - QUANTUM WIRE COUPLED TO A 1D SUPERCONDUCTOR

Finally, we discuss a possible realization of the gapless topological phase in a composite semiconducting-superconducting one-dimensional system.

Consider a semiconducting quantum wire with re-

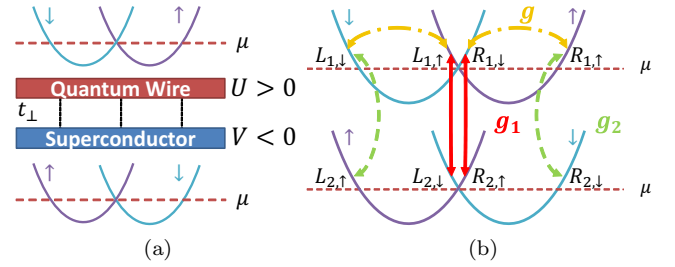


FIG. 7: (a) Realization of the topological phase in a semiconducting quantum wire with spin-orbit coupling and repulsive short-range interactions, $U > 0$, coupled to a one-dimensional superconductor with intrinsic short-range attractive interactions $V < 0$. Spin-orbit coupling is assumed to have similar magnitude and opposite sign on the two wires, and the chemical potential is taken to be such that the inner modes in both wires are at $k = 0$ to simplify the analysis. (b) Energy dispersions in the two wires and the relevant and marginal scattering processes. Two independent pair tunnelings of the inner and the outer modes are denoted by g_1 and g_2 respectively. The later is suppressed due to the mismatch in the energy dispersions for each of the spin flavors, as a result of the spin-orbit coupling. Back-scattering process due to the repulsive interactions in the semiconducting wire is denoted by g .

pulsive electron-electron interactions coupled to a one-dimensional s-wave superconductor, i.e. a wire with intrinsic attractive interactions (see Fig. 7a). This model setup can be thought of as a one-dimensional limit of the system analyzed in [25], where the 3D superconductor providing the pairing is replaced by a one-dimensional superconductor.

To simplify the analysis, we assume that each wire has a single transverse channel. We model the system as two one-dimensional electron gases, labelled by $i = 1, 2$ (the semiconducting and superconducting wires, respectively). Wire 1 has repulsive short-range density-density interactions of strength $U > 0$, and wire 2 has attractive short-range interactions of strength $V < 0$. Both wires have strong Rashba-type spin-orbit interactions. As we will argue below, a particularly favourable case for realizing the topological phase is when the spin-orbit coupling terms in the two wires have a similar magnitude and an opposite sign, such that the single-particle dispersion has the structure shown in Fig. 7a, and the chemical potential is such that the inner modes in both wires are at $k = 0$. We will focus on this case, and comment on the effects of deviation from it later. We furthermore assume that the interactions are weak, allowing for a weak-coupling renormalization group analysis.

We linearize the modes at $k = 0$ and at $k = \pm k_F$, denoting the right (left) movers with spin s in wire $i = 1, 2$ by $R(L)_{i,s} = \frac{U_{i,s}}{\sqrt{2\pi a}} e^{-i(\pm \frac{1}{2} \phi_{\rho,i} - \theta_{\rho,i} + s(\pm \frac{1}{2} \phi_{\sigma,i} - \theta_{\sigma,i}))}$, where $\phi_{\rho(\sigma),i}$ and $\theta_{\rho(\sigma),i}$ are the bosonic fields describing the

charge (spin) modes in wire $i = 1, 2$. $U_{i,s}$ are Klein factors that impose the anti-commutation relation between electrons of different spins or different wires.

In absence of tunneling between the wires, attractive interactions in the superconducting wire open a (non-topological) spin gap pinning $\phi_{\sigma,2}$ to zero. We denote the magnitude of this gap by $\Delta_{\sigma,2}$. Repulsive interactions in the semiconducting wire give rise to a backscattering term $g \left(R_{1\uparrow}^\dagger L_{1\downarrow}^\dagger R_{1\downarrow} L_{1\uparrow} + h.c. \right)$, which in terms of the bosonic fields can be written as $\frac{g}{2\pi^2 a^2} \cos(2\phi_{\sigma,1})$ (here $g > 0$ is the backscattering coupling constant). As in the usual analysis of a repulsive one-dimensional electron gas, this cosine term is marginally irrelevant and the spin sector in the semiconducting wire remains gapless.

Now consider the effect of tunneling between the wires. Due to the spin gap in the superconducting wire, single particle tunneling between the wires is suppressed at energies below the spin gap in the superconductor. Two independent pair tunneling (Josephson) processes are allowed by momentum and energy conservation (see fig. 7b). The first process describes the tunneling of a pair of electrons from the $k = 0$ modes of wire 1 to the $k = 0$ modes of wire 2. The corresponding term in the Hamiltonian is given by $R_{2\uparrow}^\dagger L_{2\downarrow}^\dagger R_{1\downarrow} L_{1\uparrow} + h.c.$. In terms of the bosonic fields it can be written as $\frac{1}{2\pi^2 a^2} \cos(2\theta_{\rho,-} + \phi_{\sigma,+})$, where we denote $\theta_{\rho,-} = (\theta_{\rho,1} - \theta_{\rho,2})$ and $\phi_{\sigma,+} = (\phi_{\sigma,1} + \phi_{\sigma,2})$. Using second-order perturbation theory in the single-particle tunnelling amplitude t_\perp , we estimate the amplitude of this term as $g_1 \sim \frac{t_\perp^2}{\Delta_{\sigma,2}}$.

Tunneling of a pair of electrons between the modes at $k = \pm k_F$ of wire 1 to either the $k = 0$ or $k = \pm k_F$ modes of wire 2 is given by $L_{2\downarrow}^\dagger R_{2\uparrow}^\dagger R_{1\uparrow} L_{1\downarrow} + h.c.$ or $R_{2\downarrow}^\dagger L_{2\uparrow}^\dagger R_{1\uparrow} L_{1\downarrow} + h.c.$; in terms of the bosonic fields these are given by $\frac{1}{2\pi^2 a^2} \cos(2\theta_{\rho,-} - \phi_{\sigma,\pm})$ respectively. These processes are suppressed with respect to the former one due to the mismatch in the energy dispersion for each of the spin flavors between the wires [52], originating from the different spin-orbit coupling in the two wires. The system is therefore required to go through an intermediate excited state at energy $\Delta_{\text{soc}} \sim m\alpha^2$, where α is the spin-orbit coupling strength. The amplitude of these scattering processes is estimated using perturbation theory in t_\perp and the interaction V as $g_2 \sim \frac{t_\perp^2 V}{\Delta_{\sigma,2} \Delta_{\text{soc}}}$.

As we will see below, there is a competition between the two kinds of Josephson processes described above. The suppression of g_2 with respect to g_1 will allow for the formation of a topological spin gap in the semiconducting wire, driving the system into the topological phase.

We are now ready to write the low-energy effective action for energies below the spin gap $\Delta_{\sigma,2}$ in the superconducting wire. Neglecting fluctuations of the field $\phi_{\sigma,2}$ and denoting all the quantities in the spin sector of the semiconducting wire simply by σ , e.g. $\phi_{\sigma,1} \rightarrow \phi_\sigma$,

the bosonized Lagrangian density takes the form $\mathcal{L} = \mathcal{L}_0 + \mathcal{L}_{\text{int}}$, where

$$\mathcal{L}_0 = \sum_{i=1,2} \frac{1}{2\pi} K_{\rho,i} \left(\frac{1}{u_{\rho,i}} (\partial_\tau \theta_{\rho,i})^2 + u_{\rho,i} (\partial_x \theta_{\rho,i})^2 \right) + \frac{1}{2\pi} \frac{1}{K_\sigma} \left(\frac{1}{u_\sigma} (\partial_\tau \phi_\sigma)^2 + u_\sigma (\partial_x \phi_\sigma)^2 \right) \quad (17)$$

is the quadratic part, with the index i running over the two wires, and

$$\mathcal{L}_{\text{int}} = \frac{1}{2\pi^2 a^2} \{ g \cos(2\phi_\sigma) + g_1 \cos(2\theta_{\rho,-} + \phi_\sigma) + g_2 \cos(2\theta_{\rho,-} - \phi_\sigma) \}. \quad (18)$$

Hereafter we denote the dimensionless couplings $\frac{g_i}{\pi a^2}$ by y_i . We normalize the units of the imaginary time such that the velocity of the spin modes u_σ is unity. We assume that the velocities of the charge modes on both wires are close to one and take the deviation $\delta u_{\rho,i} = u_{\rho,i} - 1$ to be a small parameter. This allows us to rewrite \mathcal{L}_0 as

$$\mathcal{L}_0 = \sum_{i=1,2} \frac{1}{2\pi} K_{\rho,i} (\nabla \theta_{\rho,i})^2 + \frac{1}{2\pi} \frac{1}{K_\sigma} (\nabla \phi_\sigma)^2 + \sum_{i=1,2} \frac{\delta u_{\rho,i}}{2\pi} K_{\rho,i} \left[(\partial_x \theta_{\rho,i})^2 - (\partial_\tau \theta_{\rho,i})^2 \right] \quad (19)$$

where ∇ is a 2D gradient in space-imaginary time.

We analyze the problem using weak coupling RG. In the course of the RG flow additional couplings are generated

$$\mathcal{L}_{\text{gen}} = \frac{1}{2\pi} (K_1 \nabla (\theta_{\rho,1} - \theta_{\rho,2}) \nabla \phi_\sigma + K_2 \nabla \theta_{\rho,1} \nabla \theta_{\rho,2}) \quad (20)$$

We perform the RG in real space using the operator product expansion (OPE) formalism [47]. At each RG step the short distance cutoff α is increased according to $\alpha \rightarrow (1 + dt)\alpha$ while the partition function is kept fixed by renormalizing the couplings. To second order in all couplings we obtain (see Appendix B for details):

$$\begin{aligned} \frac{dK_\sigma^{-1}}{dt} &= y^2 + \frac{(y_1^2 + y_2^2)}{4} \\ \frac{dy}{dt} &= (2 - K_\sigma) y - \frac{y_1 y_2}{2} \\ \frac{dy_1}{dt} &= \left(2 - d_{y_1} + K_1 - \frac{K_2}{2} \right) y_1 - \frac{y y_2}{2} \\ \frac{dy_2}{dt} &= \left(2 - d_{y_2} - K_1 - \frac{K_2}{2} \right) y_2 - \frac{y y_1}{2} \\ \frac{dK_{\rho 1,2}}{dt} &= y_1^2 + y_2^2 \\ \frac{dK_1}{dt} &= y_1^2 - y_2^2 \\ \frac{dK_2}{dt} &= -2(y_1^2 + y_2^2), \end{aligned} \quad (21)$$

where $d_{y_{1,2}} = (K_{\rho,1}^{-1} + K_{\rho,2}^{-1} + \frac{K_\sigma}{4})$ is the scaling dimension of the scattering processes, and the velocities do not renormalize to this order.

Note that $y_{1,2}$ are both relevant already to first order, as $d_{y_{1,2}} < 2$ for $K_\sigma, K_{\rho,1,2}$ close to their non-interacting value of two. Assuming initially $g_1 \gg g_2$, in agreement with the discussion above, y_1 flows to strong coupling first. We denote by t^* the scale at which y_1 becomes of order unity and the perturbative analysis breaks down. The other couplings are all marginal, but begin to flow significantly as t approaches t^* .

Note also the competition between $y_{1,2}$ mentioned earlier, arising due to the term $-\frac{1}{2}y y_{2(1)}$ in the beta function of $y_{1(2)}$, respectively. For $y > 0$ (repulsive interactions in the quantum wire), y_1 tends to suppress y_2 and change its sign (and vice versa). If y_1 and y_2 are initially very different in magnitude, they may end up having an opposite sign at scale $t = t^*$. Their combined contribution enhances y while keeping its sign positive. This is exactly the desired situation: in order to obtain the topological phase y has to be positive and relevant. Having $y_{1,2}$ with opposite signs is equivalent to inducing a superconducting gap with an opposite sign of the order parameter for the $k = 0$ modes with respect to the $k = \pm k_F$ ones. For a fully gapped system, such a situation is exactly what drives the system into a (gapped) topological superconducting phase in presence of time-reversal symmetry [48].

For $t \geq t^*$, we assume that $\phi_1 \equiv 2\theta_{\rho,-} + \phi_\sigma$ becomes strongly pinned to the minimum of the g_1 cosine term at π . Replacing ϕ_1 by its mean value, we obtain the following Lagrangian density:

$$\mathcal{L} = \frac{1}{2\pi} \left[\tilde{K}_{\rho,+} (\nabla \theta_{\rho,+})^2 + \frac{1}{\tilde{K}_\sigma} (\nabla \phi_\sigma)^2 - \frac{1}{4} (K_{\rho,1} - K_{\rho,2}) (\nabla \theta_{\rho,+} \nabla \phi_\sigma) + \tilde{y} \cos(2\phi_\sigma) \right], \quad (22)$$

where we ignore the contribution of the velocities $\delta u_{\rho,i}$ as they do not change the rest of the analysis. The Luttinger parameter of the total charge sector is given by $\tilde{K}_{\rho,+} = \frac{1}{4} (K_{\rho,1} + K_{\rho,2} + K_2)$. Note that this sector remains gapless as expected for a system with translational invariance. The effective parameters in the spin sector are

$$\frac{1}{\tilde{K}_\sigma} = \frac{1}{K_\sigma} + \frac{1}{16} (K_{\rho,1} + K_{\rho,2} - K_2) - \frac{1}{2} K_1 \quad (23)$$

$$\tilde{y} = y - y_2.$$

The cross term $\nabla \theta_{\rho,+} \nabla \phi_\sigma$ in the Lagrangian (22) changes the scaling dimensions of the cosine term. However, treating it perturbatively we find that it does not change the RG equations to second order. The RG flow in the spin sector for $t > t^*$ then takes the standard Kosterlitz-

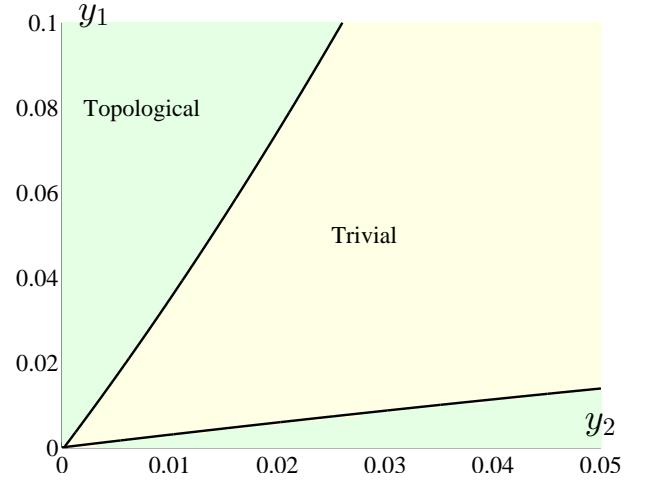


FIG. 8: Phase diagram for the composite semiconducting-superconducting one-dimensional system, as function of the bare dimensionless pair tunneling couplings $y_{1,2}(t=0)$. Initial conditions corresponding to spin-isotropic interactions in the quantum wire are used, $\frac{1}{2}K_\sigma(t=0) = 1 + y(t=0)$, where the strength of the repulsive interactions in the wire is taken to be $y(t=0) = 0.1$. We assume the non-interacting values for the charge sectors in each wire $K_{\rho,1,2}(t=0) = 2$. The scale t^* at which the integration of the RG equations (21) is stopped and the field ϕ_1 is replaced by its mean value was defined such that $y_1(t^*) = 0.5$. As argued in the text, increasing the spin-orbit coupling strength in the wires suppresses y_2 with respect to y_1 . As can be seen from the phase diagram this drives the system into the topological phase. The topological phase is obtained also for $y_2 \gg y_1$ as all the analysis is symmetric in $y_{1,2}$.

Thouless form

$$\begin{aligned} \frac{d}{dt} (\tilde{K}_\sigma^{-1}) &= \tilde{y}^2 \\ \frac{d\tilde{y}}{dt} &= (2 - \tilde{K}_\sigma) \tilde{y} \end{aligned} \quad (24)$$

The topological phase is then obtained if $\tilde{y}(t^*)$ is positive and the cosine term is relevant, i.e. if $\frac{1}{2}\tilde{K}_\sigma(t^*) < \left(\frac{1+\tilde{y}(t^*)}{1-\tilde{y}(t^*)}\right)^{1/2}$. If the cosine term is irrelevant, the spin sector remains gapless.

We can now obtain the phase diagram of the system as a function of the bare values of the pair tunnelings $y_{1,2}(t=0)$ as follows. The RG equations (21) are integrated up to the scale t^* at which y_1 reaches a value of order unity. At this scale, we replace ϕ_1 by its mean value and obtain the effective action (22). The flow continues according to Eq. 24. If the cosine term is relevant, the resulting phase is inferred from the sign of $\tilde{y}(t^*)$: $\tilde{y}(t^*) > 0$ ($\tilde{y}(t^*) < 0$) corresponds to the topological (trivial) phase, respectively.

The resulting phase diagram is shown in Fig. 8. We used initial conditions that correspond to spin-isotropic interactions in the quantum wire, $\frac{1}{2}K_\sigma(t=0) = 1 +$

$y(t=0)$. We set $y(t=0)$ to 0.1. For simplicity we assume the non-interacting values for the charge sectors in each wire $K_{\rho_{1,2}}(t=0) = 2$. The scale t^* was defined such that $y_1(t^*) = 0.5$. Neither of these choices changes the phase diagram qualitatively.

We find that the cosine term always flows to strong coupling opening a spin gap in the semiconducting wire. The topological phase is obtained for y_1 sufficiently larger than y_2 , corresponding to pair tunneling of the outer modes g_2 being suppressed with respect to the pair tunneling of the inner modes g_1 . In our microscopic system this situation can be achieved due to the form of the spin-orbit coupling in the wires. Setting the chemical potential to the point indicated in Fig. 7b is optimal for this purpose; large enough spin-orbit coupling will eventually drive the system into the topological phase, since it suppresses g_2 but not g_1 . Note that the topological phase can also be obtained for $y_2 \gg y_1$, as all the analysis is symmetric in $y_{1,2}$.

V. DISCUSSION

We have shown that a gapless topological phase, with exponentially localized edge states, can exist in a *strictly* one-dimensional time-reversal symmetric (class DIII) system with a conserved number of particles. The localization of the edge states arises due to a gap to single particle excitations in the bulk of the system. The edge states are characterized by an anomalous relation between the fermion parity and time reversal symmetry: time reversal flips the local fermion parity at the two edges, just as in the case of a DIII mean-field topological superconductor [16].

It is interesting to note that gapless topologically protected phases are possible in other symmetry classes in one dimension, as well (see, e.g., Refs. [49, 50]). In particular, class BDI (with particle-hole symmetry and time reversal that squares to $+1$) is likely to support similar phases, although there are less distinct phases than in the non-interacting case [51]. As we have shown here, as long as there is a gap for single fermion excitations in the bulk *even in the absence of long-range order*, the corresponding topological phase may be robust in a gapless one-dimensional system.

We discussed a possible realization of the phase by proximity coupling a semiconducting wire with spin-orbit coupling to a superconducting wire. Another realization of the phase may be possible in quasi-one-dimensional organic conductors where spin anisotropic interactions are believed to be present. As was analyzed in Ref. [34], these interactions could also drive the system into a phase with dominant triplet superconducting correlations, that we identified as a topological phase. In such a system, inter-chain hopping eventually drives the system into a three-dimensional long-range ordered superconducting phase;

however, if the system is very anisotropic, the properties of the topological phase (e.g., the presence of zero-energy surface states) may already be apparent at intermediate temperatures above the critical temperature, where the system is described as nearly-decoupled fluctuating one-dimensional superconductors.

It is important to note that, unlike the fully gapped topological superconducting phase which is immune to non-magnetic disorder (as long as its strength does not exceed the superconducting gap), the gapless phase can be sensitive even to weak disorder. In the topological gapless phase $2k_F$ density fluctuations are gapped. Therefore the dominant effect of an impurity potential is due to the $4k_F$ density fluctuations term. The effect of this term depends strongly on the nature of interactions in the system, parametrized by the Luttinger parameter of the charge sector, K_ρ . For K_ρ sufficiently large (in the conventions used here, $K_\rho > 1$, where $K_\rho = 2$ corresponds to a non-interacting system), backscattering due to a weak point-like impurity potential flows to zero under RG, leaving the topological phase intact. If the interactions are too strongly repulsive, corresponding to $K_\rho < 1$, any weak impurity potential becomes relevant. In the presence of many such impurities, the system becomes localized; this destroys the topological nature of the phase, and gaps out the edge states.

We conclude that the topological phase is robust in the presence of weak disorder, as long as the repulsive interactions in the system are not too strong. A metallic gate placed near the system may be used to screen the long-range part of the Coulomb interactions, thus making the topological phase more stable to disorder.

VI. ACKNOWLEDGMENTS

We would like to thank Liang Fu, Arbel Haim, Yuval Oreg, Yoni Schattner, Ady Stern, Yochai Werman, and Konrad Wölms for fruitful discussions. We are particularly indebted to Miles Stoudenmire for his help with setting up the DMRG calculations using the ITensor package. This research was supported by the Minerva foundation, a Minerva ARCHES prize, a Marie Curie CIG grant, a GIF-Young Researcher grant, and by the Israel Science Foundation.

Appendix A: Tunneling density of states at an edge of a gapless topological system

In this section we describe the calculation of the matrix element given in Eq. 9, which contributes to the $\omega \rightarrow 0$ tunneling density of states (TDOS) for a system in the gapless topological phase.

Consider a topological region that extends from $x = 0$ to $x = L$, with a trivial region on its either side. The

bosonized Hamiltonian describing the system is given by

$$H = \int dx \sum_{\alpha=\rho,\sigma} \frac{u_\alpha}{2\pi} \left[K_\alpha (\partial_x \theta_\alpha)^2 + \frac{1}{K_\alpha} (\partial_x \phi_\alpha)^2 \right] + \int dx \frac{g(x)}{2\pi^2 a^2} \cos(2\phi_\sigma), \quad (\text{A1})$$

where $g(x) = g > 0$ in the topological region $0 < x < L$, and $g(x) = g_0 < 0$ in the trivial regions, $x \leq 0$ and $x \geq L$. We assume the couplings g, g_0 are large enough such that ϕ_σ is pinned close to the minimum of the potential in each region. This allows us to expand the cosine around $\pi n_{1,2}$ in the trivial regions and around $\pi(m + \frac{1}{2})$ in the topological region, where $n_{1,2}, m$ are integers. We consider a variational Hamiltonian where the cosine term is replaced with a quadratic potential, consistent with such an expansion. There are two distinct configurations of the potential, corresponding to different states:

$$V_0(x) = \frac{1}{2\pi^2 a^2} \begin{cases} -2g_0 \phi_\sigma^2 & x < 0, x > L \\ 2g(\phi_\sigma - \frac{\pi}{2})^2 & 0 < x < L \end{cases}$$

and

$$V_1(x) = \frac{1}{2\pi^2 a^2} \begin{cases} -2g_0(\phi_\sigma - \pi)^2 & x < 0 \\ 2g(\phi_\sigma - \frac{\pi}{2})^2 & 0 < x < L \\ -2g_0 \phi_\sigma^2 & x > L \end{cases}$$

The respective variational Hamiltonians are denoted by $H_{0,1}$ and their ground states by $|0\rangle$ and $|1\rangle$. Saddle point configurations of ϕ_σ in these states, $\phi_{\sigma,0,1}(x)$, are depicted in Fig. 1. We denote the difference between them by $\Delta\phi_\sigma = \phi_{\sigma,1} - \phi_{\sigma,0}$. Note that the energy of the spin sector for these two configurations is the same, and they are therefore nearly degenerate. The difference in energy arises due to the charging energy (which scales as $\frac{1}{L}$, tending to zero for large enough system), as in the state $|1\rangle$ the total spin in the system is $\frac{1}{2}$, corresponding to an odd number of particles, while in the state $|0\rangle$ the total number of particles is even. Since the density of the particles in the system is given by $-\frac{1}{\pi}\partial_x \phi_\rho$, the respective saddle point configurations of ϕ_ρ in these two states differ by a constant gradient term $\Delta\phi_\rho = \pi(1 - \frac{x}{L})$ in the region $0 < x < L$. The two ground states are therefore related by a unitary transformation $|1\rangle = e^{-i\hat{\delta}}|0\rangle$, where $\hat{\delta} = \sum_{\alpha=\rho,\sigma} \hat{\delta}_\alpha$ and

$$\hat{\delta}_\alpha = \frac{1}{\pi} \int_{-\infty}^{\infty} dx' \Delta\phi_\alpha(x') \partial_{x'} \theta_\alpha(x').$$

To see this note that under this transformation the field $\phi_\alpha \rightarrow \phi_\alpha + \Delta\phi_\alpha$.

The matrix element that is expected to give the largest contribution to the TDOS at $\omega \rightarrow 0$ can now be written as

$$\langle 1 | \Psi_\uparrow^\dagger(x) | 0 \rangle = \langle e^{i\hat{\delta}} \Psi_\uparrow^\dagger(x) \rangle,$$

where an expectation value with respect to the ground state of H_0 is assumed in the final expression. Writing the single particle creation operator as

$$\Psi_\uparrow^\dagger(x) \sim \sum_r e^{-irk_F x} e^{i\phi_{r,\uparrow}},$$

where $\phi_{r,\uparrow} = \frac{1}{2}r\phi_\rho(x) - \theta_\rho(x) + \frac{1}{2}r\phi_\sigma(x) - \theta_\sigma(x)$ and the sum over $r = \pm 1$ stands for right and left movers respectively, the matrix element becomes

$$\langle e^{i\hat{\delta}} \Psi_\uparrow^\dagger(x) \rangle \sim \sum_r e^{-irk_F x} \langle e^{i\hat{\delta}} e^{i\phi_{r,\uparrow}} \rangle.$$

To proceed we therefore need to diagonalize H_0 and find the expansion of the bosonic fields $\phi_{\rho,\sigma}$ and $\theta_{\rho,\sigma}$ in terms of its eigenmodes. Note that since the spin and charge sectors are decoupled, the expectation value above can be written as a product

$$\langle e^{i\hat{\delta}} e^{i\phi_{r,\uparrow}} \rangle = \prod_{\alpha=\rho,\sigma} \langle e^{i\hat{\delta}_\alpha} e^{i(\frac{1}{2}r\phi_\alpha(x) - \theta_\alpha(x))} \rangle_\alpha,$$

where $\langle \dots \rangle_{\alpha=\rho,\sigma}$ denotes the expectation value in the ground state of the charge and spin sectors respectively.

We begin by diagonalizing the spin sector, $H_{0,\sigma}$. For simplicity we take the spin gap in the trivial regions to be infinite, $|g_0| \rightarrow \infty$ (equivalently we can assume that the topological region is surrounded by vacuum). This pins the field ϕ_σ and the current $\partial_x \theta_\sigma$ at the boundary to zero, i.e. $\phi_\sigma|_{x=0,L} = 0$ and $\partial_x \theta_\sigma|_{x=0,L} = 0$. A mode expansion for the fields $\phi_\sigma, \theta_\sigma$ then takes the following form:

$$\theta_\sigma(x) = i \sum_{k=1}^{\infty} \sqrt{\frac{1}{K_\sigma k}} \cos\left(\frac{\pi k x}{L}\right) (a_k - a_k^\dagger) \\ \phi_\sigma(x) = \phi_{\sigma,0}(x) + \sum_{k=1}^{\infty} \sqrt{\frac{K_\sigma}{k}} \sin\left(\frac{\pi k x}{L}\right) (a_k + a_k^\dagger)$$

where the expansion for ϕ_σ is around the constant saddle point solution $\phi_{\sigma,0}(x)$, and a_k^\dagger, a_k are bosonic creation and annihilation operators satisfying the commutation relations $[a_k, a_{k'}^\dagger] = \delta_{k,k'}$.

The Hamiltonian translates into

$$H_{0,\sigma} = \frac{1}{2} \sum_{k=1}^{\infty} \left[A_k (a_k a_k^\dagger + a_k^\dagger a_k) + B_k (a_k^2 + a_k^{\dagger 2}) \right]$$

where $A_k = u_\sigma \frac{\pi k}{L} + \frac{|g|K_\sigma}{\pi a^2} \frac{L}{\pi k}$, $B_k = \frac{|g|K_\sigma}{\pi a^2} \frac{L}{\pi k}$, and a Bogoliubov transformation $a_k = \alpha_k b_k + \beta_k b_k^\dagger$ can be used to bring it into a diagonal form

$$H_{0,\sigma} = \sum E_k b_k^\dagger b_k + \text{const.}$$

The coefficients in the transformation are $\alpha_k = \sqrt{\frac{1}{2} \left(\frac{A_k}{E_k} + 1 \right)}$, $\beta_k = -\sqrt{\frac{1}{2} \left(\frac{A_k}{E_k} - 1 \right)}$. The eigen-energies

are given by $E_k = \sqrt{A_k^2 - B_k^2}$ and b_k^\dagger, b_k are the bosonic creation and annihilation operators of the corresponding eigen-modes.

The fields $\phi_\sigma, \theta_\sigma$ are given by linear combinations of these creation and annihilation operators. Hence, the expectation value can be calculated using the identity

$$\left\langle e^{i\hat{\delta}_\sigma} e^{i(\frac{1}{2}r\phi_\sigma(x) - \theta_\sigma(x))} \right\rangle_\sigma = e^{-\frac{1}{2}\langle (\hat{\delta}_\sigma + \frac{1}{2}r\phi_\sigma(x) - \theta_\sigma(x))^2 \rangle_\sigma}.$$

Denote the spin gap in the system by $\Delta_\sigma = \sqrt{\frac{2|g|u_\sigma K_\sigma}{\pi a^2}}$ and the inverse correlation length by $\kappa = \xi^{-1} = \Delta_\sigma/u_\sigma$. In the limit $|g_0| \rightarrow \infty$ the difference between the saddle point configurations is

$$\Delta\phi_\sigma = \begin{cases} \pi & x < 0 \\ \pi \frac{\sinh[\kappa(L-x)]}{\sinh(\kappa L)} & 0 < x < L \\ 0 & x > L \end{cases}.$$

We can then write $\hat{\delta}_\sigma = \theta_\sigma(0) + \Delta\theta_\sigma$, where $\Delta\theta_\sigma = \int_0^L dx e^{-\kappa x} \partial_x \theta_\sigma(x)$ for $\kappa L \gg 1$. Note also that we are interested only in the absolute value of the matrix element. The expectation values $\langle \phi_\sigma(x) \theta_\sigma(x) \rangle$ and $\langle \phi_\sigma(x) \hat{\delta}_\sigma \rangle$ are imaginary and only contribute a constant phase shift to the oscillations in $2k_F$ of the matrix element squared. The asymptotic behavior is dictated by the function

$$F_\sigma \equiv \left\langle \left(\theta_\sigma(x) - \hat{\delta}_\sigma \right)^2 \right\rangle + \frac{1}{4} \langle \phi_\sigma^2(x) \rangle.$$

Denoting $\gamma_k = \left(1 + \kappa^2 / \left(\frac{\pi k}{L}\right)^2\right)^{1/2}$ we obtain

$$F_\sigma = \frac{1}{K_\sigma} \sum_{k=1}^{\infty} \frac{\gamma_k}{k} \left[\cos\left(\frac{\pi k x}{L}\right) - \frac{\kappa^2}{\kappa^2 + \left(\frac{\pi k}{L}\right)^2} \right]^2 + \frac{1}{4} K_\sigma \sum_{k=1}^{\infty} \frac{1}{k \gamma_k} \sin^2\left(\frac{\pi k x}{L}\right).$$

Taking the continuum limit $\frac{1}{L} \rightarrow 0$, the sum over k can be written as an integral over $q = \frac{\pi k}{L}$. Performing the integral and considering the asymptotics for $\xi \ll x \ll L$ we find that

$$F_\sigma \sim \frac{\pi}{2} \frac{1}{K_\sigma} \kappa x.$$

A similar calculation for the charge sector gives the following asymptotic behavior for $a \ll x \ll L$

$$F_\rho \equiv \left\langle \left(\theta_\rho(x) - \hat{\delta}_\rho \right)^2 \right\rangle + \frac{1}{4} \langle \phi_\rho^2(x) \rangle \sim \frac{1}{2} \left(\frac{1}{K_\rho} + \frac{1}{4} K_\rho \right) \ln\left(\frac{x}{a}\right) + \frac{1}{K_\rho} \ln\left(\frac{L}{a}\right).$$

The absolute value of the matrix element squared is therefore

$$\left| \left\langle e^{i\hat{\delta}} \Psi_\uparrow^\dagger(x) \right\rangle \right|^2 \sim e^{-(F_\sigma + F_\rho)} \sim \left(\frac{a}{L}\right)^{\frac{1}{K_\rho}} \left(\frac{a}{x}\right)^{\frac{\alpha}{2}} e^{-\frac{\pi}{2K_\sigma} \frac{x}{\xi}},$$

where we denote $\alpha = \frac{1}{K_\rho} + \frac{1}{4} K_\rho$ and $\xi = \frac{u_\sigma}{\Delta_\sigma}$ is the correlation length.

Appendix B: RG flow equations obtained using the operator product expansion

In this appendix we give further details on the derivation of the RG flow equations (21). As mentioned in the main text, we perform the RG in real space. At each step we rescale the short distance cutoff α , defined as the minimal distance between two operators in the theory, according to $\alpha \rightarrow (1 + dt)\alpha$. We use the operator product expansion (OPE) to replace pairs of operators which are within the new short distance cutoff, allowing us to recover the original action with renormalized couplings.

The general form for an OPE of two operators O_i, O_j is

$$: O_i(r_1) : : O_j(r_2) := \sum_k C_{ijk}(r_1 - r_2) : O_k\left(\frac{r_1 + r_2}{2}\right) :,$$

where $: O_i :$ denotes normal ordering of the operator. The equality is valid only when both sides of the equation are considered inside a correlation function with another operator (or set of operators) at a distance much greater than $|r_1 - r_2|$ from the operators $O_{i,j}$. The functions $C_{ijk}(r_1 - r_2)$ have the form $C_{ijk} = \frac{c_{ijk}}{|r_1 - r_2|^{d_i + d_j - d_k}}$, where $d_{i,j,k}$ are the scaling dimensions of the corresponding operators and c_{ijk} are the OPE coefficients which are pure numbers. The beta functions to second order of the respective couplings $g_{i,j,k}$ are then given by [47]

$$\frac{dg_k}{dt} = (d - d_k) g_k - \sum_{i,j} c_{ijk} g_i g_j,$$

where d is the dimension of the problem.

We demonstrate the OPE explicitly for the pair of operators $O_1 = \nabla \theta_{\rho,-} \nabla \phi_\sigma$ and $O_2 = \cos(2\theta_{\rho,-} + \phi_\sigma)$, both of which we treat perturbatively. We start by writing the cosine as a sum of exponents, and expanding the exponent as a series

$$: e^{i(2\theta_{\rho,-} + \phi_\sigma)} := \sum_n \frac{i^n}{n!} : (2\theta_{\rho,-} + \phi_\sigma)^n := \sum_n \frac{i^n}{n!} \sum_m \binom{n}{m} 2^m : \theta_{\rho,-}^m \phi_\sigma^{n-m} :$$

The normal ordered product of the operators $:O_1(r_1)::O_2(r_2):$ will then contain a summation over terms of the form

$$:\partial_i\theta_{\rho,-}(r_1)\partial_i\phi_\sigma(r_1)::\theta_{\rho,-}^m(r_2)\phi_\sigma^{n-m}(r_2):.$$

In each such term, we can contract $\partial_i\theta_{\rho,-}(r_1)$ with one of the $\theta_{\rho,-}(r_2)$, giving m possible configurations. For each of them, there are $n-m$ ways to contract $\partial_i\phi_\sigma(r_1)$ with one of the $\phi_\sigma(r_2)$. These contractions are given by

$$\langle\partial_i\phi_\sigma(r_1)\phi_\sigma(r_2)\rangle = -\frac{1}{2}K_\sigma\frac{(r_1-r_2)_i}{|r_1-r_2|^2}$$

and

$$\begin{aligned}\langle\partial_i\theta_{\rho,-}(r_1)\theta_{\rho,-}(r_2)\rangle &= \\ \langle\partial_i\theta_{\rho,1}(r_1)\theta_{\rho,1}(r_2)\rangle + \langle\partial_i\theta_{\rho,2}(r_1)\theta_{\rho,2}(r_2)\rangle &= \\ -\frac{1}{2}(K_{\rho,1}^{-1} + K_{\rho,2}^{-1})\frac{(r_1-r_2)_i}{|r_1-r_2|^2}\end{aligned}$$

respectively. The product of the operators now becomes

$$:\nabla\theta_{\rho,-}\nabla\phi_\sigma::e^{i(2\theta_{\rho,-}+\phi_\sigma)}:=\frac{1}{4}K_\sigma(K_{\rho,1}^{-1}+K_{\rho,2}^{-1})\frac{1}{|r_1-r_2|^2}\sum_n\frac{i^n}{n!}\sum_m\binom{n}{m}2^mm(n-m):\theta_{\rho,-}^{m-1}\phi_\sigma^{n-m-1}:.$$

Rewriting the sum over m as

$$\begin{aligned}2n(n-1)\sum_m\binom{n-2}{m-1}:(2\theta_{\rho,-})^{m-1}\phi_\sigma^{n-2-(m-1)}:= \\ 2n(n-1):(2\theta_{\rho,-}+\phi_\sigma)^{n-2}:\end{aligned}$$

and the sum over n as

$$2i^2\sum_n\frac{i^{n-2}}{(n-2)!}:(2\theta_{\rho,-}+\phi_\sigma)^{n-2}:= -2:e^{i(2\theta_{\rho,-}+\phi_\sigma)}:$$

we obtain

$$\begin{aligned}:\nabla\theta_{\rho,-}\nabla\phi_\sigma::\cos(2\theta_{\rho,-}+\phi_\sigma):= \\ -\frac{1}{2}K_\sigma(K_{\rho,1}^{-1}+K_{\rho,2}^{-1})\frac{1}{|r_1-r_2|^2}:\cos(2\theta_{\rho,-}+\phi_\sigma):,\end{aligned}$$

where we identify $-\frac{1}{2}K_\sigma(K_{\rho,1}^{-1}+K_{\rho,2}^{-1})$ as the OPE coefficient. This results in the following contribution to the beta function of y_1

$$\frac{dy_1}{dt} = \frac{1}{2}K_\sigma(K_{\rho,1}^{-1}+K_{\rho,2}^{-1})K_1y_1.$$

To second order in the coupling constants, we can use the non-interacting values for the Luttinger parameters $K_\sigma = K_{\rho,1,2} = 2$ and write

$$\frac{dy_1}{dt} = K_1y_1.$$

[1] For a general discussion of this question, see: P. Bonder-son and C. Nayak, Physical Review B **87**, 195451 (2013).

- [2] N. Read and D. Green, *Phys. Rev. B* **61**, 10267 (2000).
- [3] A. Kitaev, in *AIP Conf. Proc.*, Vol. 1134 (2009) p. 22.
- [4] S. Ryu, A. P. Schnyder, A. Furusaki, and A. W. W. Ludwig, *New Journal of Physics* **12**, 065010 (2010).
- [5] G. E. Volovik, *The universe in a helium droplet* (Oxford University Press, 2009).
- [6] M. Hasan and C. Kane, *Reviews of Modern Physics* **82**, 3045 (2010).
- [7] X.-L. Qi and S.-C. Zhang, *Reviews of Modern Physics* **83**, 1057 (2011).
- [8] A. Y. Kitaev, *Physics-Uspekhi* **44**, 131 (2001).
- [9] Y. Oreg, G. Refael, and F. von Oppen, *Phys. Rev. Lett.* **105**, 177002 (2010).
- [10] R. M. Lutchyn, J. D. Sau, and S. Das Sarma, *Phys. Rev. Lett.* **105**, 077001 (2010).
- [11] J. Alicea, *Rep. Prog. Phys.* **75**, 076501 (2012).
- [12] C. Beenakker, *Annual Review of Condensed Matter Physics* **4**, 113 (2013).
- [13] L. Fidkowski, R. Lutchyn, C. Nayak, and M. Fisher, *Phys. Rev. B* **84**, 195436 (2011).
- [14] J. Sau, B. Halperin, K. Flensberg, and S. Das Sarma, *Phys. Rev. B* **84**, 144509 (2011).
- [15] J. Ruhman, E. Berg, and E. Altman, arXiv preprint arXiv:1412.3444 (2014).
- [16] X.-L. Qi, T. L. Hughes, S. Raghu, and S.-C. Zhang, *Phys. Rev. Lett.* **102**, 187001 (2009).
- [17] L. Fu and E. Berg, *Phys. Rev. Lett.* **105**, 097001 (2010).
- [18] S. Deng, L. Viola, and G. Ortiz, *Phys. Rev. Lett.* **108**, 036803 (2012).
- [19] S. Nakosai, Y. Tanaka, and N. Nagaosa, *Phys. Rev. Lett.* **108**, 147003 (2012).
- [20] B. Seradjeh, *Phys. Rev. B* **86**, 121101(R) (2012).
- [21] C. L. M. Wong and K. T. Law, *Phys. Rev. B* **86**, 184516 (2012).
- [22] F. Zhang, C. L. Kane, and E. J. Mele, *Phys. Rev. Lett.* **111**, 056402 (2013).
- [23] S. Nakosai, J. C. Budich, Y. Tanaka, B. Trauzettel, and N. Nagaosa, *Phys. Rev. Lett.* **110**, 117002 (2013).
- [24] A. Keselman, L. Fu, A. Stern, and E. Berg, *Phys. Rev. Lett.* **111**, 116402 (2013).

- [25] A. Haim, A. Keselman, E. Berg, and Y. Oreg, *Phys. Rev. B* **89**, 220504 (2014).
- [26] E. Gaidamauskas, J. Paaske, and K. Flensberg, *Phys. Rev. Lett.* **112**, 126402 (2014).
- [27] X.-J. Liu, C. L. M. Wong, and K. T. Law, *Phys. Rev. X* **4**, 021018 (2014).
- [28] K. Wölms, A. Stern, and K. Flensberg, *Phys. Rev. Lett.* **113**, 246401 (2014).
- [29] Y. X. Zhao and Z. D. Wang, *Phys. Rev. B* **90**, 115158 (2014).
- [30] T. Giamarchi, *Quantum physics in one dimension* (2004).
- [31] A. Altland and M. R. Zirnbauer, *Physical Review B* **55**, 1142 (1997).
- [32] A. Luther and V. J. Emery, *Phys. Rev. Lett.* **33**, 589 (1974).
- [33] If the higher order cosine terms (higher harmonics) are relevant, the transition can become first order, or there could be an intermediate phase in which time reversal symmetry is spontaneously broken. However, a smooth crossover from the $g < 0$ to the $g > 0$ phase is not possible.
- [34] T. Giamarchi and H. J. Schulz, *Phys. Rev. B* **33**, 2066 (1986).
- [35] Giamarchi, T. and Schulz, H.J., *J. Phys. France* **49**, 819 (1988).
- [36] F. Pollmann, A. M. Turner, E. Berg, and M. Oshikawa, *Phys. Rev. B* **81**, 064439 (2010), [arXiv:0910.1811 \[cond-mat.str-el\]](#).
- [37] A. M. Turner, F. Pollmann, and E. Berg, *Phys. Rev. B* **83**, 075102 (2011), [arXiv:1008.4346 \[cond-mat.str-el\]](#).
- [38] L. Fidkowski and A. Kitaev, *Phys. Rev. B* **83**, 075103 (2011).
- [39] X. Chen, Z.-C. Gu, and X.-G. Wen, *Phys. Rev. B* **83**, 035107 (2011), [arXiv:1008.3745 \[cond-mat.str-el\]](#).
- [40] X. Chen, Z.-C. Gu, and X.-G. Wen, *Phys. Rev. B* **84**, 235128 (2011), [arXiv:1103.3323 \[cond-mat.str-el\]](#).
- [41] N. Schuch, D. Pérez-García, and I. Cirac, *Phys. Rev. B* **84**, 165139 (2011), [arXiv:1010.3732 \[cond-mat.str-el\]](#).
- [42] S. B. Chung, J. Horowitz, and X.-L. Qi, *Phys. Rev. B* **88**, 214514 (2013).
- [43] S. R. White, *Phys. Rev. Lett.* **69**, 2863 (1992).
- [44] S. R. White, *Phys. Rev. B* **48**, 10345 (1993).
- [45] U. Schollwöck, *Annals of Physics* **326**, 96 (2011).
- [46] Calculations were performed using the ITensor Library, <http://itensor.org/>.
- [47] J. Cardy, *Scaling and renormalization in statistical physics*, Vol. 5 (Cambridge University Press, 1996).
- [48] X.-L. Qi, T. L. Hughes, and S.-C. Zhang, *Phys. Rev. B* **81**, 134508 (2010).
- [49] J. P. Kestner, B. Wang, J. D. Sau, and S. Das Sarma, *Phys. Rev. B* **83**, 174409 (2011).
- [50] F. Iemini, L. Mazza, D. Rossini, S. Diehl, and R. Fazio, *ArXiv e-prints* (2015), [arXiv:1504.04230 \[cond-mat.str-el\]](#).
- [51] L. Fidkowski and A. Kitaev, *Phys. Rev. B* **81**, 134509 (2010), [arXiv:0904.2197 \[cond-mat.str-el\]](#).
- [52] Here, we have assumed that the tunnelling process conserves the spin.